Bichromatic force measurements using atomic beam deflections

M. R. Williams, F. Chi, M. T. Cashen, and H. Metcalf
Department of Physics and Astronomy, State University of New York, Stony Brook, New York 11794-3800
(Received 21 July 1999; published 12 January 2000)

The spontaneous decay rate γ of excited atomic states limits the radiative force on atoms to $\hbar k\gamma/2$. This bottleneck in the dissipative exchange of momentum between atoms and light can be overcome by coherent control of the momentum exchange interactions. The bichromatic force provides such control by using stimulated instead of spontaneous emission to produce the force, while at the same time exploiting spontaneous emission to enable a dissipative interaction. It is implemented with two counterpropagating light beams, each containing two frequencies, whose phases, amplitudes, and frequency difference are carefully chosen. We have made precise measurements of the extremely large magnitude and velocity range of this bichromatic force, and have shown that its velocity dependence near the edge of its range is suitable for atomic beam slowing and laser cooling. Our measurements have corroborated various models and calculations of this bichromatic force.
PACS number(s): 32.80.Pj, 42.50.Vk

I. INTRODUCTION

In the early days of laser cooling, the view of two-level atoms moving in a monochromatic laser beam provided the elementary picture. The topics that could be described this way included atomic beam slowing and cooling, optical molasses, optical dipole traps, lattices and band-structure effects, and a host of others. Within a few years, however, it became clear that this simple view was inadequate, and that the multiple level structure of atoms was necessary to explain some experiments.

Perhaps the most dramatic impact came from the discovery of cooling below the Doppler temperature $T_D \equiv \hbar\gamma/2k_B$ [1], where k_B is Boltzmann's constant and $\gamma \equiv 1/\tau$ is the natural width of the optical transition. This could only be explained by polarization gradient cooling in atoms with multiple ground-state levels. Other examples requiring such multiple atomic levels are the magneto-optic trap (multiple excited state levels) and velocity-selective coherent population trapping (multiple ground-state levels).

Thus the extension from two-level to multilevel atoms gave an unexpected richness to the topic of atomic motion in optical fields. It seems natural to expect that a comparable multitude of new phenomena is to be found for the motion of two-level atoms in multifrequency fields, but this subject has not received as much attention.

In the Doppler cooling process of two-level atoms, it is the radiative force that produces *both* the slowing force *and* the dissipation necessary for cooling. The force arises from the incoherent sequence of absorption followed by spontaneous emission. Thus it is limited to $F \leqslant \hbar k\gamma/2$, where $k \equiv 2\pi/\lambda$ and λ is the wavelength of the optical cooling transition.

By contrast, in most cases of laser cooling in multilevel atoms, such as Sisyphus cooling in a polarization gradient, it is the dipole force that works on the atoms. This force is usually present in multiple beams of monochromatic light such as standing waves. Since this force results from the rapid coherent sequence of absorption followed by stimulated emission, it does not suffer from such limits. Although this force can be very strong, its sign alternates in space on the wavelength scale, and thus its spatial average vanishes. Moreover, this force is completely conservative so its cooling aspect, or velocity dependence, must arise from the relatively infrequent spontaneous emission events, and so such sub-Doppler cooling forces are similarly limited to a magnitude of $\hbar k\gamma/2$. Thus not only is the cooling aspect of the dipole force limited in strength, but also the spatial average of the strong conservative component vanishes.

There have been two independent proposals that used two frequencies to provide spatial rectification of the dipole force [2,3], and thus make the use of such strong forces practical. These exploit beams of different intensities and detunings to provide a rectified force, and during the following few years there were some experiments that demonstrated this idea [4–6]. Then in 1997 there was a dramatic demonstration of the use of a bichromatic field with two beams of equal intensities and detunings that provided both a strong force and wide velocity range [7]. Using only modest laser power, these authors demonstrated that this bichromatic force could decelerate a thermal beam of Cs to ~ 20 m/s in just a few cm with no Doppler compensation.

Unlike the limited velocity range of the previously described rectified dipole force, the bichromatic force has both a very large velocity range v_b and magnitude F_b. Since the force covers a much larger range of velocities, Doppler compensation using a multikilowatt Zeeman tuning magnet, for example, is rendered unnecessary for slowing a thermal beam. Not only is the velocity range v_b very much larger than the usual velocity range for slowing forces of $\gamma/2k$, but also it has a strong velocity dependence at its range boundaries so that it can cool. Naturally this (dissipative) velocity dependence originates from the occasional spontaneous emission events at a rate determined by γ, but the magnitude of the force is not limited by this rate. Thus it is a valuable method for fast, short-distance deceleration of thermal atoms that minimizes atom loss, thereby making it a most useful and important tool in the production of cold, dense atomic samples for traps, lithography, and other purposes.

Here we report careful, detailed measurements of the velocity dependence of this force to $\sim 5\%$ accuracy that demonstrate its extremely large magnitude and strong velocity dependence [8], features that distinguish it from the radiative forces used for laser cooling for the past 20 years. We have

measured F_b to be $\cong 5$ times larger than the maximum possible values achievable with the radiative force [9]. Furthermore, this factor of 5 is imposed only by our laser power: the bichromatic force has no simple, fundamental limit to either F_b or v_b. These measurements support calculations that include the π-pulse model first suggested in [2] and presented in [7], dressed atom pictures in two different bases [10,11], and direct numerical integration of the optical Bloch equations (OBE) [12].

II. THE BICHROMATIC FORCE

A. Qualitative Discussion

The π-pulse model for describing bichromatic forces provides an intuitive notion of how it works. Consider atomic motion along the axis of counterpropagating bichromatic light beams. Each beam contains the same two frequencies, and they are detuned from atomic resonance by $\pm\delta$ (difference frequency $= 2\delta$). Each beam can be described as an amplitude-modulated single-carrier frequency at the atomic resonance frequency ω_a having modulation period π/δ, and δ is chosen such that $\pi/\delta \ll \tau$. The equal intensities of each beam are chosen so that the envelope of one ''pulse'' of the beats satisfies the condition of a π pulse for the atoms: ground-state atoms are coherently driven to the excited state and vice versa. In terms of the on-resonance Rabi frequency, this condition is $\Omega = \pi\delta/4$, where $\Omega \equiv \gamma\sqrt{I/2I_s}$, and $I_s \equiv \pi hc/(3\lambda^3\tau)$ (Ω is the on-resonance Rabi frequency associated with each frequency component of each beam).

Atoms in this light field are subject to these π pulses alternately from one beam direction and then from the other, so the force on them can become very large. This is because the first π pulse causes excitation along with momentum transfer in one direction, and the second counterpropagating π pulse causes stimulated emission producing a momentum transfer *along the same direction as the first pulse*. Similar forces have been demonstrated using ps π pulses on Cs [13].

Thus atoms are coherently driven between the ground and excited states, and momentum is monotonically exchanged with the light field. The magnitude of the momentum transfer in each cycle is $2\hbar k$ and the repetition rate of these controlled processes is δ/π, so that the optimum total force is on the order of $2\hbar k\delta/\pi$. This is *very* much larger than the usual maximum Doppler force $\hbar k\gamma/2$, principally because it is a coherently controlled rapid momentum exchange whose rate is limited only by laser power through the π-pulse condition. The bichromatic force is *not* subject to saturation.

The mechanism described above requires two additional features to be applicable to atomic beam slowing: (1) there must be some directional asymmetry because the excitation pulse could come from either direction, and thus the force could point either way, and (2) it must be velocity dependent so that it can compress the phase space volume of the atomic sample.

The first condition is satisfied by a careful choice of the relative intervals between the counterpropagating ''pulses'' of light (i.e., the relative phase of the modulation), and exploitation of the random nature of spontaneous emission. If the ''pulses'' are evenly spaced, spontaneous emission spoils the cycle described above since an excited atom can spontaneously decay to the ground state so that the next pulse causes absorption rather than stimulated emission. Thus each spontaneous emission produces a reversal in the direction of the force, resulting in zero average force.

However, if the pulses are timed unevenly so that they come in closely spaced pairs, one from each direction, their asymmetry indeed produces a ''preferred'' direction. When the first pulse of each closely spaced pair produces excitation, the atom spends less time in the excited state before stimulated emission by the second pulse, resulting in a lower probability for spontaneous emission that would reverse the force. Just the opposite situation prevails for an atom excited by the second pulse of a ''pair,'' because spontaneous emission is more likely to occur in the longer interval than in the shorter one when $\tau \gg \pi/\delta$. While it is still possible for an atom to get into a cycle that will produce a force in either direction, atoms that get out of phase with the preferred order by suffering spontaneous emission during the short interval are more likely to undergo correction than to remain out of phase, so there will be more events that produce a force in the direction of travel of the leading pulse. This model was experimentally realized in Ref. [13] on Cs by the use of ps π pulses from a pulsed laser.

The optimum phase difference between the beats in the counterpropagating beams is found from our numerical calculations to be $\cong \pi/4$, so that atoms typically experience a force in the wrong direction for 25% of their time. Then the same 25% is needed to negate this undesired force, leaving 50% of the time for the desired force. Thus the average force is $\hbar k\delta/\pi$, half the optimum estimated above, and this is also borne out by the numerical calculations of Refs. [7,10,14].

The second condition requires simultaneous consideration of both the light shift *and* the Doppler shift, and the simplified picture of π pulses given above is insufficient. Instead, a dressed state description of atoms moving in a bichromatic, time-dependent field is required. We are currently working on the development of this difficult and interesting problem.

B. Quantitative discussion

We have done calculations by direct numerical integration of the OBE using the program provided by the authors of Refs. [7,12]. The resulting values of $F_b(v)$, plotted as a solid line in Fig. 1 for various values of the phase and the ratio Ω/δ, show the characteristic behavior of the bichromatic force. The general progression shown in the various panels of Fig. 1 is unchanged even with variations of δ/γ and Ω/γ. Figure 1 also shows that $F_b(v)$ spans approximately $\pm\delta/2k$.

Our numerical calculations show that F_b and v_b are both proportional to δ (this is also supported by the π-pulse model above). Thus the time t_b required to change atomic velocities by v_b is independent of δ. More generally, $t_b = \eta(Mv_b/F_b) = \pi\eta/2\omega_r$ is the time required to change velocities by a fixed fraction $\eta \leqslant 1$ of v_b, where $\omega_r \equiv \hbar k^2/2M$ is the recoil frequency. For the Rb transition at $\lambda = 780$ nm, where $\omega_r \approx 2\pi \times 3.8$ kHz, $t_b \approx 60\eta\ \mu$s. In our experiment, the competition between readily measurable de-

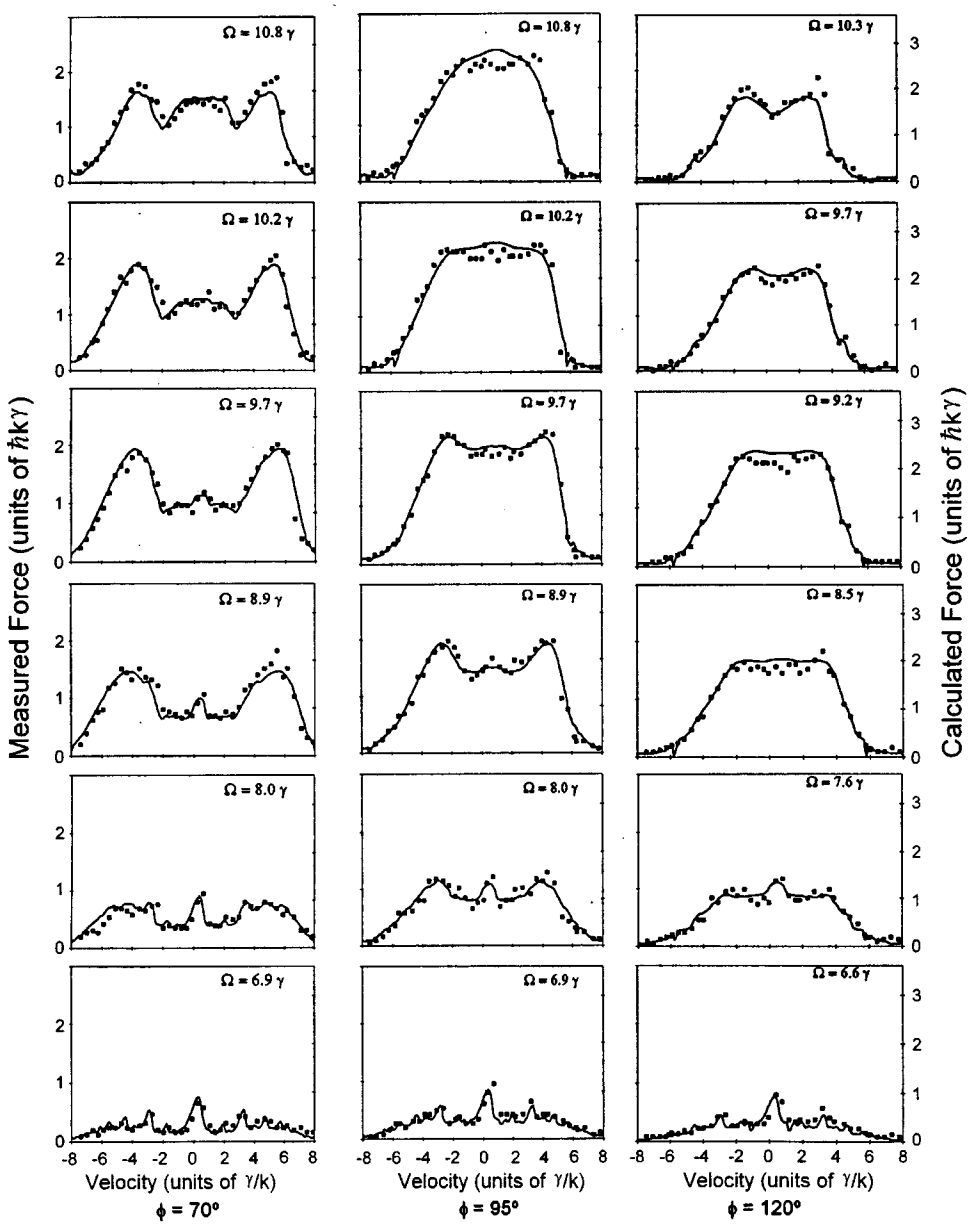

FIG. 1. Each panel shows the velocity dependence of the bichromatic force. The three columns correspond to phases of 70°, 95°, and 120°. The solid curves are calculated by direct numerical integration of the OBE and then convolved with the experimental resolution. The measured values are shown as points (uncertainties are $\pm\hbar k\gamma/10$, about the size of the symbols). For these data, $\delta=2\pi\times 55$ MHz$=9.1\gamma$, but the appearance of the curves in the sequence changes very little for different values of δ as long as the ratios δ/γ and Ω/γ are preserved. The ratios of the different values of Ω were chosen by a half-wave plate and polarizer combination, starting with the maximum value in (a) of 10.8γ, and decreasing by the factors 0.95 in (b), 0.90 in (c), 0.83 in (d), 0.74 in (e), and 0.64 in (f) from Ω_{max}. The calculation and experiment have vertical scales different by the factor 0.83 in all panels. Note that the π-pulse condition $\Omega=\pi\delta/4\approx 7.2\gamma$ would fall between the bottom two rows.

flection and suitable resolution of the force led to the choice $\eta=0.25$, but we have varied it from 0.04 to 0.4. With $\eta=1$, a typical thermal Rb atomic beam at 300 m/s can be brought to rest in less than 1 cm.

The required light intensity I can be estimated from v_b using the π-pulse condition, or inferred from our numerical calculations (see Fig. 1) that suggest $\Omega\simeq\delta$ is more appropriate than $\Omega=\pi\delta/4$. Then $I\equiv 2(\Omega/\gamma)^2 I_s\simeq 2(\delta/\gamma)^2 I_s$, where $I_s\simeq 1.67$ mW/cm^2 for the Rb transition we use. Thus the required power can be determined from v_b appropriate to an experiment and the geometrical conditions that determine the laser beam size. Throughout this work we have used $\gamma=2\pi\times 6.065$ MHz [15].

III. APPARATUS

A. Bichromatic field

The light field is produced by a Ti:Sapphire laser tuned to drive the $(F,M_F)=(2,2)\rightarrow(3,3)$ transition in ^{87}Rb and the $(3,3)\rightarrow(4,4)$ transition in ^{85}Rb. For ^{85}Rb, the beam passes

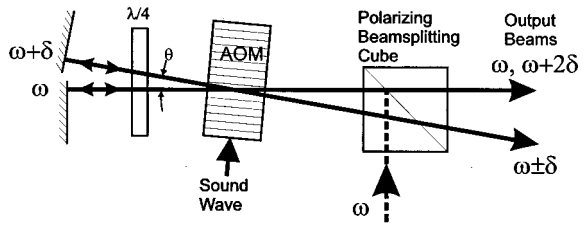

FIG. 2. The incoming laser beam shown as a broken line at frequency ω enters the AOM and is Bragg diffracted with 50% efficiency into an outgoing beam. The emerging beams have equal power, and frequencies $\omega+\delta$ and ω. Both are retroreflected back to the AOM, and it splits each of them again, producing beams as shown (the quarter-wave plate and polarizing beam splitter serve to extract the two final beams). With $\delta=2\pi\times 55$ MHz, $\theta\approx 12$ mrad.

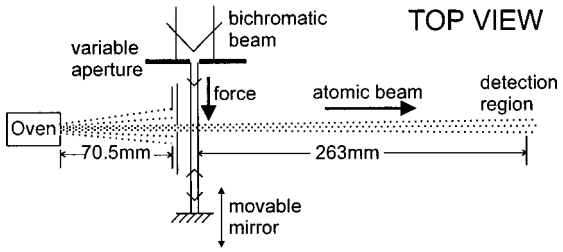

FIG. 3. Atoms emerge from the oven at the left, are vertically collimated by the wide horizontal slit, and then well collimated by the 190-μm vertical slit. In the interaction region they cross the laser beams that exert the bichromatic force in the direction shown by the arrow for about 6 mm, and then they fly freely to the detection region.

through a 2.9-GHz electro-optic modulator (EOM) to impose a weak hyperfine structure (hfs) repumping frequency on it. The other EOM sideband is ignored. The beam is then directed to an AOM where the frequencies for the bichromatic fields are produced using an AOM as described below. The large hfs of ^{87}Rb allows sufficient spectroscopic resolution so that the repumping is not necessary.

It is sometimes desirable to arrange for the force to act from $v=\delta/k\equiv v_b$ to $v=0$, and this is readily implemented by upshifting both of the frequencies in one of the counterpropagating beams and downshifting those in the other beam [7]. If the shifts are $\pm\delta/2$, the picture given in Sec. II A is correct in a frame moving at speed $v_b/2$ in the laboratory, which shifts the horizontal axis of Fig. 1 by the desired amount. However, this results in the requirement for four distinct laboratory frequencies.

Making the four frequencies is accomplished with a single AOM as shown in Fig. 2. The incoming laser beam (broken line) at frequency ω_l is Bragg reflected with 50% efficiency into an outgoing beam at $\omega_l+\delta$, while the remaining 50% of the power has frequency ω_l. Both of these beams are retroreflected back to the AOM, and it splits each of them again, producing four frequencies as shown (the two beams retracing the input beam are separated with a polarizing beam splitter and quarter wave plate). These four laboratory-frame frequencies exactly satisfy the criteria for a strong bichromatic force in a frame moving at $v=\delta/2k$, so that the force acts on laboratory velocities ranging from $v=\delta/k$ to $v=0$, precisely what is needed for beam slowing or collimation. In our deflection experiments reported here, we have used each pair of these frequencies as the bichromatic beam (using the retroreflector) or both pairs in a counterpropagating configuration.

The AOM not only shifts the carrier but also the sidebands produced by the EOM. Thus, associated with each of the frequencies generated by the AOM (ω_l, $\omega_l\pm\delta$, and $\omega_l+2\delta$) there is also a frequency that can contribute to repumping. In both the four-frequency experiment (because of four distinct frequencies) and the two-frequency experiment (because of the retroreflection) there is the possibility for atoms with four different transverse velocities to experience on-resonant repumping for each repumping transition. Because both the $F_g=2\rightarrow F_e=2$ and $F_g=2\rightarrow F_e=3$ transitions can accomplish repumping, this leads to a maximum of eight different transverse velocities being repumped. In our parameter range we have resonant repumping on four of these independent velocities that are spaced throughout the velocity distribution.

For the two-frequency case, the relative phase of the ''pulses'' of the counterpropagating light beams is determined by the distance from the atomic beam to the retroreflecting mirror (see Fig. 3). For the four-frequency case it is determined by the relative distances between the AOM and the interaction region. For our typical values of detuning $\delta/2\pi\sim 55$ MHz, the round-trip distance for a 2π phase shift is $c(\pi/\delta)\sim 2.7$ m.

B. The atomic beam

An overall top view of our apparatus is shown in Fig. 3. The beam from an oven at $T\approx 450$ K with a circular aperture of diameter 330 μm is vertically collimated by an LN_2-cooled, 800-μm-high horizontal slit 70.5 mm away, and then by a 190-μm-wide vertical slit that is 3 mm from this horizontal slit. This vertical slit can be moved transversely by 20 mm to choose various beam directions. (In some cases we have used an array of eight such slits 2 mm apart to enable multiple simultaneous measurements.) About 8 mm beyond the vertical slit, the atoms enter an interaction region where the Earth's field is canceled to ± 3 μT, and the field can be varied to ± 300 μT in any direction. The length of this interaction region d is typically limited by apertures to the central 6 mm of the expanded bichromatic laser beams where their intensities are quite uniform ($2\times$beam waist$=18$ mm). After accounting for the diffraction of these apertures, the residual error is quite small.

After the interaction region the atoms fly freely for $D=26.3$ cm, and then their horizontal positions are measured by optical absorption in the detection region. Here the ^{87}Rb (^{85}Rb) atoms are subject to two (three) separate laser beams as shown in Fig. 4. The first beam, the ''pumper,'' is used only for ^{85}Rb. It is vertical and is tuned to the $F_g=2\rightarrow F_e=3$ transition to optically pump the atoms into the $F_g=3$ hfs ground-state sublevel. The second one, the ''modulator,'' is tuned near the $F_g=2$ (3)$\rightarrow F_e=1$ (2) transition

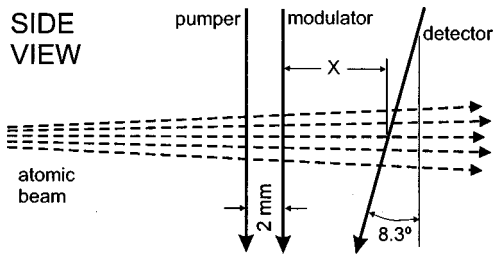

FIG. 4. The three lasers used for longitudinal velocity-selective detection of ^{87}Rb (^{85}Rb). The pumper is used only for ^{85}Rb and is tuned from the $F_g=2\rightarrow F_e=3$ transition to optically pump all the atoms into the $F_g=3$ hfs ground state. The modulator is modulated at 3 kHz by >100 MHz and is tuned near the $F_g=2\ (3)\rightarrow F_e=1\ (2)$ transition to empty the $F_g=2\ (3)$ state. The detector is tuned to the $F_g=2\ (3)\rightarrow F_e=3\ (4)$ cycling transition. Its angle with the atomic velocity is $\pi/2+8.3°$ as shown in the figure. The inconsequential distance x varies linearly between 2 and 12 mm (due to the three-dimensional detection geometry) as the detector beam is transversely scanned.

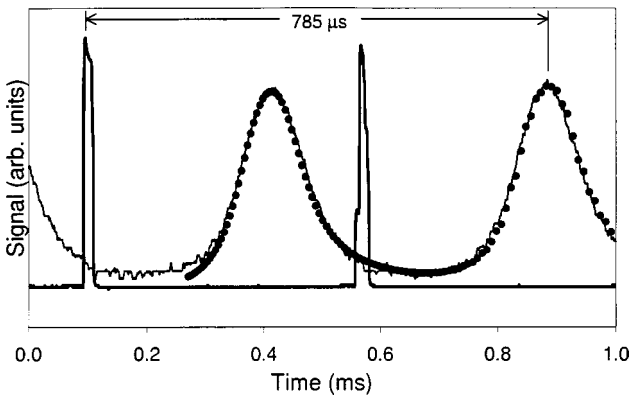

FIG. 5. The optical pumping, time-of-flight measurement. A laser beam in the interaction region is pulsed on and off (narrow pulses) and tuned to optically pump atoms into the detected ground state. The arrival of the optically pumped atoms in the detection region, in this case 27.4 cm downstream, is subsequently detected (broad peaks). The pulse of atoms on the far right actually arises from the light pulse on the far left. The symbols represent the expected atom signal based on the beam geometry and the other experimental parameters, and their good fit to the data is consistent with our assumed velocity distribution. The only free parameters were the amplitude of the signal and the angle of the detection laser (taken to be 98.3°).

and its frequency is modulated over a range of >100 MHz at a rate of 3 kHz to modulate the population of the $F_g=2\ (3)$ state to enable lock-in detection. The third one, the ''detector,'' is directed at 98.3° to the atomic beam axis for velocity selection, and is tuned to the $F_g=2\ (3)\rightarrow F_e=3\ (4)$ transition. Its absorption by atoms in the beam is measured.

All three laser beams are transversely scanned across the atomic beam by an oscillating mirror to map out the atomic beam's spatial profile. A large lens directs the detection beam onto a photocell from any position in its scan range. The transverse velocity change caused by the bichromatic force is determined from the physical shift Δx in the horizontal position of the absorption peak(s) that is (are) measured by the spatially scanned detection laser. The atoms are subject to a bichromatic force of magnitude determined by their transverse velocity (see Fig. 1) that acts for a time dependent on their longitudinal velocities and the interaction length d. We measure their displacement, and when this is combined with their selected longitudinal velocities, the resultant deflection angle gives the average force on them.

The geometry fixes the width of the undeflected atomic beam(s) at this point at 1 mm, and the detection laser beam is a 510-μm-wide image of a slit, resulting in a transverse velocity resolution of $\simeq\pm0.5$ m/s. The accessible width of the detection region is 8 cm, making more than 50 spatial regions or transverse velocity steps available. The power broadened width from the detection laser is about 10 MHz. The longitudinal velocity is selectable by the frequency of the detection laser at a 98.3° angle; our experiments span the range of 250–400 m/s. Including the spread of vertical velocities, the resulting longitudinal velocity resolution is ±30 m/s (see Fig. 5). Thus the interaction time spread ranges from $\cong15\%$ to $\cong25\%$, with a central uncertainty $<5\%$.

Since the magnitude of the measured force depends on the square of the longitudinal velocity selected by the detection laser, and since this velocity is determined by the Doppler shift at the selected angle according to $v_{/\!/}=\delta_d/(k\cos\theta)$, the accuracy of θ is very important (here δ_d is the detuning of the detection laser). The geometry of our detection region is restricted to $90°\leqslant\theta\leqslant98°$, and because of the correspondingly small Doppler shift, a small error can have important consequences.

Our best determination of the angle θ was done using an optical pumping–time-of-flight technique with ^{85}Rb. An independent diode laser was sent through an AOM and the first-order beam was directed to follow the path of the bichromatic beams through the interaction region. This diffracted beam was resonant with the $F_g=2\rightarrow F_e=3$ transition, causing atoms to be optically pumped to the $F_g=3$ state. The rf drive power to the AOM was pulsed on and off, and the corresponding arrival times of the optically pumped atoms at the detection laser were recorded (see Fig. 5). This time delay between the pulsing of the light and the arrival of the optically pumped atoms, combined with the distance to the detection laser, was used to determine the longitudinal velocity of the detected atoms to about 0.7%, and thus the angle θ to ±1 mrad.

IV. RESULTS

A. Measurements

We have measured the bichromatic force for a range of values of many independent parameters including detuning, phase, light intensity, applied magnetic field, interaction length, longitudinal velocity, laser beam configuration, and isotope. Each of these parameters could be independently varied. A typical example of the raw data showing eight peaks both with and without the bichromatic force is shown in Fig. 6. Each of these corresponds to a different transverse

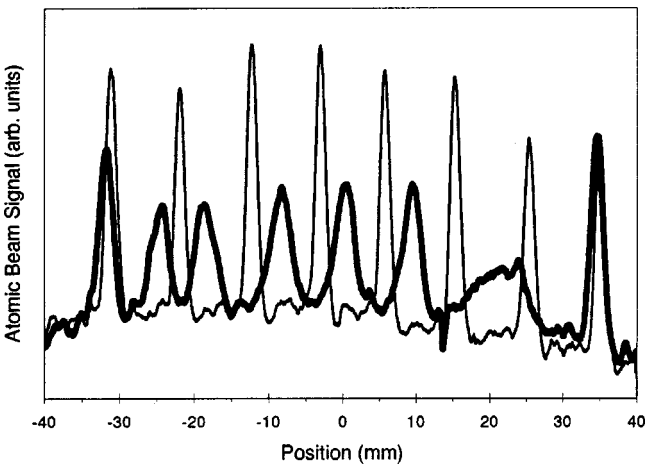

FIG. 6. Typical raw data showing the atomic beam positions without (thin line) and with (thick line) the bichromatic force. The force is acting toward the left. The integrated signal of the initial and deflected beams are the same to within a few percent. For these data, $\delta=9.1\gamma$, $\phi=90°$, and $\Omega=8.9\gamma$. Note that not all the peaks are moved by equal amounts since the force is velocity dependent. The peaks on either end are outside the range of the force, so they are not moved at all, and the second one from the right one is considerably smeared because its velocity spans the sharp edge of the force-vs-velocity curve.

velocity, and so the displacement of each of them is a measure of the force at each of these velocities. The array of slits can be moved to measure the force for velocities spaced between these eight peaks, and several such data sets provide one of the panels shown in Fig. 1.

We found that overall the best measurements could be done using the most abundant isotope ^{85}Rb, and for these measurements we needed hfs repumping. In Fig. 1 the numerical calculations are plotted as solid lines for comparison with the measurements done with an interaction length of approximately 6 mm, $\delta/2\pi=55$ MHz, and detection of atoms with a longitudinal velocity of 350 m/s. Data taken with these parameters for the three different phases $\phi=65°$, 90°, and 115° are plotted as points in Fig. 1. The different values of Ω were obtained with a half-wave plate and a polarizer, and thus proportionality is assured. Both the solid lines and the measurements are shifted to the right and show a small asymmetry because they are plotted against the initial velocity, and each single measurement necessarily spanned a range of a few m/s to achieve a readily measurable displacement Δx. The only adjusted parameter in the calculations is Ω_{max}, and it is chosen to best match the shape and magnitude trends of the data. The measured intensity I corresponds to within a few percent to this value of $2\Omega_{max}^2 I_s/\gamma^2$.

We also used the four frequencies in two beams (ω_l, $\omega_l+2\delta$, and $\omega_l\pm\delta$) put out by the AOM. With $\omega_l=\omega_a-\delta/2$, the bichromatic force can be made to push all atoms between v_b and 0 toward $v=0$. Since the position in the detection region for atoms with transverse velocity $v=0$ is the same for all longitudinal velocities, even non-velocity-selective data show a single, narrow pile up of atoms at $v=0$, as expected.

In all our experiments, the measured force is consistently smaller than the calculated one, so a scaling factor has been used between the vertical axes on each side of Fig. 1 for the best match. We found this factor to be 0.83 ± 0.02 for ^{85}Rb (plotted in Fig. 1), and 0.79 ± 0.02 for ^{87}Rb. (It is interesting to note that the maximum force measured by the authors of Ref. [13] was also $\approx$80% of the anticipated value.) An isotopic difference could be caused by variations in the optical pumping among the Zeeman and hfs levels of the two isotopes. For the ^{87}Rb data we do no hfs optical pumping because its larger hfs allows adequate spectroscopic resolution. Thus the ^{87}Rb measurements were done on only those atoms that emerged from the source in the $(F,M_F)=(2,2)$ sublevel, or were optically pumped very quickly in the circularly polarized bichromatic light, and remained there throughout the interaction region. By contrast, the ^{85}Rb measurements were done in the presence of the continuous repumping light produced by one of the sidebands of the EOM as discussed above.

B. Discussion of results

Figure 1 shows detailed agreement between the data and the characteristic progression of the calculated force curves as Ω is varied, confirming that the intensity measurements are correct. That is, the frequency δ is derived from a synthesizer so it is well known. Thus the plots of Fig. 1 provide a direct comparison between Ω and δ, and these are consistent with our measurements. The measured force is calculated from $F_{meas}=Mv_l^2(\Delta x)/Dd$, where v_l is the selected longitudinal velocity. Thus F_{meas} depends only on three measured distances and v_l^2, and does not depend on quantities that are more difficult to determine such as the Rabi frequency Ω.

In the retroreflected beam, two-frequency experiment, the phase is determined geometrically by the distance d_ϕ between the atomic beam and the retroreflecting mirror and is given by $\phi=4d_\phi\delta/c$. We found that the data were better fitted with phase shifts 5° larger than those determined by the distance to the retromirror. At least three factors act to shift the phase from this value. The first is the additional path length through the 1-cm-thick window, which adds $\approx1°$ to the phase. The second arises from the dispersion of the residual Rb vapor in the atomic beam chamber, which acts to reduce the phase. This dispersion effect was tested in two ways. (1) Using a small Michelson interferometer with a Rb absorption cell in one arm, we scanned a diode laser through the Rb resonance and measured the fringe shift. (2) We calculated that a $-4°$ shift along the 20-cm round-trip path between the atomic beam and the exit window can be caused by a Rb vapor pressure of 3.4×10^{-8} Torr ($\sim$1/10 of the room-temperature vapor pressure). This seems reasonable in our vacuum. The third could arise from a reflection of the bichromatic beam from the exit window of the vacuum system. The window is a shorter distance from the atomic beam than the retroreflecting mirror and thus a reflection from it would have a smaller ϕ. The window is antireflection coated and thus only produces a weak reflection that when com-

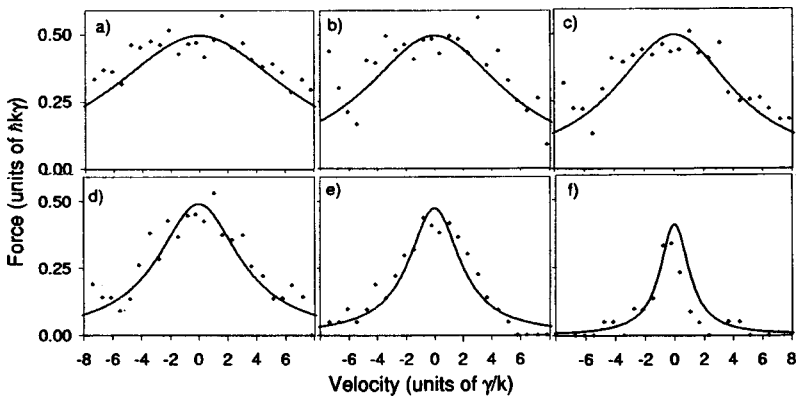

FIG. 7. The force from a single frequency traveling-wave laser beam that is on-resonance with the $v=0$ atoms was measured as a function of intensity. The saturation parameter s of the laser beam in panel (a)–(f) is 233, 140, 93, 47, 18, and 4.4, respectively. The data points represent the measured force and the smooth line is the calculation (not a fit since there are no free parameters). The uncertainties here are about the same $\pm\hbar k\gamma/10$ as in Fig. 1, but the scale size is different so the scatter appears larger.

bined with the main retroreflected beam acts to give a small negative contribution to the phase.

We have made many independent tests to search for systematic errors that could produce the $\simeq 20\%$ discrepancy between the measurements and the numerical calculations. One of these was measurements on ^{87}Rb (using no repumper) to check the effects of optical pumping, where we found essentially no difference from the ^{85}Rb data. The signal-to noise ratio S/N was worse because we used only that small fraction of the oven output that was in the $(F,M_F)=(2,2)$ sublevel of this less abundant isotope.

In still another test, we reversed the direction of the force by simply changing the phase of the beats between the counterpropagating beams by 180°. This purely geometric test again showed no difference in the magnitude of the force.

Although the bichromatic force is maximized for symmetric detuning ($\omega_a \pm \delta$), the effect of an asymmetric shift ($\omega_a + \delta_{\rm asym} \pm \delta$) was also measured. There are two important features that we found from these measurements. (1) The force is relatively insensitive to $\delta_{\rm asym}$ over a range of about 1γ for $\delta \approx 9\gamma$, and (2) the maximum of the force was measured to be near $\delta_{\rm asym}=0$, in agreement with the numerical calculations. Moreover, this indicates that the tuning of the laser frequency is indeed well known, and that the laser frequency instability and linewidth ($<\gamma/2$) are insignificant.

We have also applied a dc magnetic field in the interaction region to see what effects it might have. Not surprisingly, we found that varying the field to ± 300 μT along the direction of the $\vec{k}$ vectors of the circularly polarized bichromatic laser beams produced virtually no effect. However, even 120 μT perpendicular to the $\vec{k}$ vectors reduced the force by a factor of 2 from its zero field maximum. This is surprising because the Larmor frequency is only $\gamma/10$ (since $g_F=1/3$), and this is small compared to every frequency in the system. Even the Rabi frequency for the weak repumping beam is approximately γ. We plan further investigation of this result.

As a final check, we have done a direct optical force calibration with the Doppler force in order to check our entire measurement scheme. We deflected the atoms with a single frequency traveling-wave laser beam whose intensity could be made sufficiently high that the force was truly $\hbar k\gamma/2$, and used the same data acquisition method to measure its velocity dependence, which is characterized by significant power broadening. As shown in Fig. 7 the calculated and measured forces agree very well (both magnitude and width) over a large range of s.

V. CONCLUSIONS

We feel that the discrepancy between F_{meas} and the calculated forces of about 20% is caused by a number of small contributions. Clearly one of these arises from the readily visible effects of atmospheric turbulence on the laser beam that travels 15 m through a pipe from the laser table to the AOM (a fiber is impractical because of the incoupling power loss). When we choose the best Ω_{max} to fit the data, it represents some average value. The turbulence causes fluctuations that differ for the two frequencies of the bichromatic laser beam. This creates an intensity mismatch of the beams that can only lower the force.

Another beam intensity effect arises from the loss of light associated with the imperfect transmission of the window traversed twice by the retroreflected beam. In addition, absorption by the residual cloud of Rb vapor mentioned above further unbalances the counterpropagating beams. Each of these independently can reduce the measured force by a few %.

Still another effect arises from optical pumping. In the case of ^{87}Rb where we use no repumper and lose those atoms that fall into the $F=1$ ground state, there is still an initial optical pumping among the Zeeman levels as the atoms enter the circularly polarized bichromatic laser beams. In the case of ^{85}Rb where optical pumping occurs (there is almost no signal without the repumper), the atoms still spend some of their time in the $F=2$ ground state where they experience no force.

Because of its potential for a huge magnitude and velocity range, along with the strong velocity dependence at the range boundaries, this force will enable atomic beam slowing and cooling in a new domain of parameters. It is particularly well suited for decelerating metastable $^3S_1$ He atoms at $\lambda = 1083$ nm, especially with the advent of fiber amplifiers that generate more than 1 W of $\lambda = 1083$ nm light. He atoms with initial velocity of 1000 m/s can be brought to rest in less than 1 cm. This is truly a remarkable result.

Another attractive application is atomic beam collimation, since the large velocity range would enable a large capture angle. This would enhance the production of very intense, high flux atomic beams. Consider an atomic beam entering a

bichromatic Gaussian laser beam transversely as shown in Fig. 3. Suppose that the peak laser intensity corresponds to $\Omega = 10.2\gamma$ in the middle column of Fig. 1. As atoms enter the Gaussian beam at the 3/4 intensity region, they experience a force as shown in the panel for $\Omega = 8.9\gamma$, which is very nearly the maximum for those with large transverse velocities. Thus the ''capture'' range for collimation by bichromatic light is enhanced by the peaks in the force near the ends of the velocity range.

To conclude, we have performed careful and detailed measurements of the bichromatic force. With our parameters, we have found it to be more than five times the magnitude of the Doppler force (limited only by the available laser power) and to have velocity-dependent details that agree extremely well with the calculations.

ACKNOWLEDGMENTS

This work was supported by ONR and ARO.

[1] P. Lett *et al.*, Phys. Rev. Lett. **61**, 169 (1988).
[2] V.S. Voitsekhovich *et al.*, Pis'ma Zh. Éksp. Teor. Fiz. **49**, 138 (1989) [JETP Lett. **49**, 161 (1989)]; Zh. Éksp. Teor. Fiz. **99**, 219 (1991) [Sov. Phys. JETP **72**, 219 (1991)].
[3] A.P. Kazantsev and I. Krasnov, J. Opt. Soc. Am. B **6**, 2140 (1989); see also Pis'ma Zh. Éksp. Teor. Fiz. **46**, 333 (1987) [JETP Lett. **46**, 420 (1987)].
[4] R. Grimm *et al.*, Phys. Rev. Lett. **65**, 1415 (1990).
[5] R. Gupta *et al.*, Phys. Rev. Lett. **71**, 3087 (1993).
[6] T. Grove *et al.*, Phys. Rev. A **51**, R4325 (1995).
[7] J. Söding *et al.*, Phys. Rev. Lett. **78**, 1420 (1997). Note that, in this work, $\gamma \equiv 1/2\tau$.
[8] M. Williams *et al.*, Phys. Rev. A **60**, R1763 (1999).
[9] More recently we have measured the bichromatic force by deflecting a beam of metastable He with $\lambda = 1.083$ μm light from a model no. 30 dBm fiber amplifier made by Optocomm, 22304 Lannion, France. We found $F_b = 20\hbar k\gamma$, a factor of 40 larger than the maximum radiative force.
[10] R. Grimm *et al.*, Opt. Lett. **19**, 658 (1994).
[11] H. Metcalf, Bull. Am. Phys. Soc. **43**, 1365 (1998); M. Williams *et al.*, in *Abstracts of the XVI, International Conference Proceedings on Atomic Physics, Windsor, Ontario, 1998* (University of Windsor, Windsor, Ontario, 1998), p. 448.
[12] J. Söding, Ph.D. thesis, University of Heidelberg 1996 (unpublished).
[13] A. Goepfert *et al.*, Phys. Rev. A **56**, R3354 (1997).
[14] R. Grimm *et al.*, in Proceedings of the International School of Physics ''Enrico Fermi,'' course CXXXI, Varenna, 1996, edited by A. Aspect, W. Barletta, and R. Bonifacio (IOS Press, Amsterdam, 1996), p. 481; as in Ref. [7], $\gamma \equiv 1/2\tau$.
[15] U. Voltz and H. Schmoranzer, Phys. Scr. **T65**, 48 (1996).